NAVAL SHIP RESEARCH AND DEVELOPMENT CENTER
Bethesda, Maryland 20034

GENERATION AND PROPAGATION OF VORTICITY UNDER THE PERFECT-SLIP CONDITION

HANS J. LUGT

COMPUTATION AND MATHEMATICS DEPARTMENT

February 1972 Report 3794

GENERATION AND PROPAGATION OF VORTICITY UNDER THE PERFECT-SLIP CONDITION

The Naval Ship Research and Development Center is a U. S. Navy center for laboratory effort directed at achieving improved sea and air vehicles. It was formed in March 1967 by merging the David Taylor Model Basin at Carderock, Maryland with the Marine Engineering Laboratory at Annapolis, Maryland.

Naval Ship Research and Development Center
Bethesda, Md. 20034

MAJOR NSRDC ORGANIZATIONAL COMPONENTS

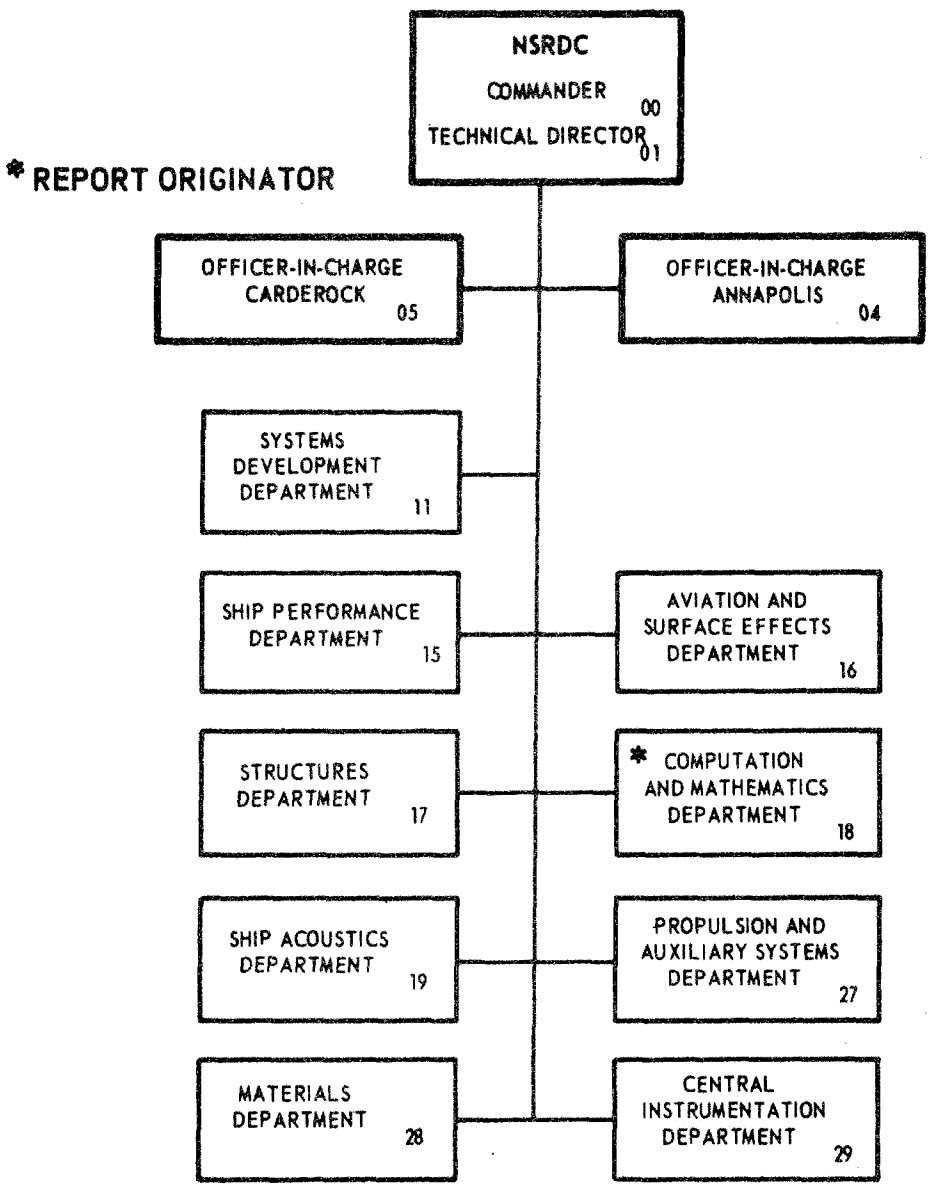

DEPARTMENT OF THE NAVY

NAVAL SHIP RESEARCH AND DEVELOPMENT CENTER

Bethesda, Maryland 20034

GENERATION AND PROPAGATION OF VORTICITY UNDER THE PERFECT-SLIP CONDITION

by

HANS J. LUGT

February 1972

Report 3794

TABLE OF CONTENTS

LIST OF FIGURES

NOTATION

a	Focal distance of the elliptic body contour
A, B	Integration constants defined in Equation (5)
C_D	Drag coefficient
C_{DP}, C_{DF}	Drag coefficient due to pressure, friction
C_L	Lift coefficient
C_M	Moment coefficient
d	Width = $2a \cosh \eta_1$
n, s	Intrinsic coordinates
p'	Pressure
p	Dimensionless pressure = $p' / U^2\rho$
r, ϕ λ	Spherical polar coordinates
Re	Reynolds number = dU/ν
t'	Time
t	Dimensionless time = $t'U/a$
$\bar{t}$	Dummy variable
u	Velocity component along streamline
U	Constant velocity far away from the body
x, y	Cartesian coordinates
α	Angle of attack
η, θ	Elliptic coordinates defined by Equation (13)
κ	Curvature of streamlines
μ, ν	Dynamic, kinematic viscosity
ξ	$= r/\sqrt{\nu t'}$
ρ	Density
τ	Shear stress along streamline
ψ	Stream function
ω'	Vorticity
ω	Dimensionless vorticity = $\omega' a/U$

ABSTRACT

Renewed interest in slip flow within the realm of continuum physics has resulted in a numerical study on generation and propagation of vorticity in a flow past thin elliptic cylinders under the perfect-slip condition. Computer results show that surface vorticity is more concentrated at the edges for perfect slip than for nonslip, due to the surface curvature. Flow separation, instability, and vortex shedding occur also under the perfect-slip condition. Although drag is drastically reduced for slender body configurations, drag coefficients for a plate normal to the flow are almost the same for nonslip and perfect slip, at least for Reynolds number 10. All computations were carried out for Reynolds numbers below 200.

ADMINISTRATIVE INFORMATION

This study was funded by the Naval Ship Systems Command under the Mathematical Sciences Program, Subproject SR0140301.

The German translation of this report will be published in a special issue of the Deutsche Luft- und Raumfahrt series (May 1972) which is dedicated to Prof. Alfred Walz on the occasion of his 65th birthday. Prof. Walz played an active part in the history of this project (see Acknowledgments).

REMARKS ON THE GENERATION OF VORTICITY

Current experiments[1] on special solid-surface treatment which may prevent fluids from adhering to the surface of solid bodies have prompted a study of the fluid dynamic implications of flows under the perfect-slip condition. This type of motion must be distinguished from the slip flow known in rarefied gas dynamics, where the mean free path lengths of the gas molecules are considered to be of the order of the body dimension. Here, perfect-slip flow is investigated within the framework of continuum physics, that is, the mean free path length is very small with respect to the body length. Still, the adherence properties must be explained on the molecular level, and they enter the flow theory of a continuum only as boundary conditions. This paper does not discuss the cause of nonslip and does not describe methods of producing slip flow. Rather it deals with the change in the flow behavior when the nonslip condition is replaced by the perfect-slip condition. The solution to this problem is not only of engineering interest but furnishes additional insight into the generation and propagation of vorticity. The latter aspect is stressed in this study.

In an incompressible homogeneous fluid, which is not subjected to nonconservative forces, vorticity can be created only at the boundaries of the fluid. For a body moving in a fluid at rest at infinity, vorticity is thus produced at the body surface. For simplicity we restrict ourselves to plane and axisymmetric flows and use the intrinsic coordinates s and n, where n denotes the arc length along streamlines, and n is orthogonal to s.[2] $n = n_1$ represents the surface of the body. With u and τ designating the velocity component and the shear stress along the streamlines, the nonslip and perfect-slip conditions at the surface are defined by

1. References are listed on page 15

$$n = n_1 : \quad u \equiv 0, \qquad \text{Nonslip} \tag{1}$$

$$\tau \equiv 0, \ \mu \neq 0, \qquad \text{Perfect-Slip} \tag{2}$$

where μ is the dynamic viscosity.

The amount of vorticity produced at the surface is determined by the velocity field. Vorticity defined as the curl of the velocity vector is

$$\omega' = -\frac{\partial u}{\partial n} + \kappa u. \tag{3}$$

The shear stress in terms of u is

$$\tau = -\mu \left(\frac{\partial u}{\partial n} + \kappa u\right), \tag{4}$$

where κ designates the curvature of the surface. In plane motions ω' is the vorticity component normal to the plane; in axisymmetric flows ω' is the azimuthal component. Under the nonslip condition, Equation (1), vorticity and shear stress at the surface are $\omega' = \tau/\mu = -\partial u/\partial n$, whereas the perfect-slip condition, Equation (2), requires $\omega' = 2\kappa u = -2\partial u/\partial n$. Hence, under the perfect-slip condition vorticity can only occur when the curvature κ is nonzero.

SLOW MOTION AROUND A SPHERE

Vorticity generation and diffusion under either nonslip or perfect slip may be illustrated by the closed-form solution for the flow past a sphere at vanishing Reynolds number. This well-known solution consists of two parts; one, called the Stokeslet, deals with the vorticity distribution and the other, a potential flow, satisfies the boundary conditions. The potential flow consists of a dipole and a parallel flow.

$$\psi = -\frac{U}{2} \sin^2\phi \left(Ar + \frac{B}{r} + r^2\right), \tag{5}$$

$$\omega' = U \sin\phi \frac{A}{r^2}, \quad r \neq 0. \tag{6}$$

Here, ψ is the stream function in the spherical polar coordinate system (r, ϕ, λ), and U is the uniform flow velocity far from the body. The radius of the sphere is unity. The constants A and B are at our disposal to fulfill the boundary conditions on the sphere's surface.

A remarkable connection exists between dipole and Stokeslet. In a dipole vorticity is concentrated at the singularity r = 0. If this source-sink ceases to produce vorticity at the time t' = 0, the dipole decays according to

$$\psi_D = - UB \frac{\sin^2\phi}{r} \left[\operatorname{erf} \left(\frac{\xi}{2}\right) - \frac{\xi}{\sqrt{\pi}} e^{-\xi^2/4} \right], \tag{7}$$

$$\omega_D' = \frac{1}{4\sqrt{\pi}} UBr \sin\phi \, (\nu t')^{-5/2} e^{-\xi^2/4}, \tag{8}$$

where $\xi = r/\sqrt{\nu\, t'}$ and ν is the kinematic viscosity. Equation (9) was found by Phillips[3], Equation (8) by the author[4]. If the dissipating dipole is integrated over time, the accumulation of vorticity results in,

$$\psi_s = - \int_o^{t'} \psi_D \, (t' - \bar{t}) \, d\bar{t}$$

$$= - \frac{U}{2} Br \sin^2\phi \left[1 - (1 - \frac{2}{\xi^2}) \operatorname{erf} \left(\frac{\xi}{2}\right) - \frac{2}{\xi\sqrt{\pi}} e^{-\xi^2/4} \right], \tag{9}$$

$$\omega_s' = UB \frac{\sin\phi}{r^2} \left[1 - \operatorname{erf} \left(\frac{\xi}{2}\right) + \frac{\xi}{\sqrt{\pi}} e^{-\xi^2/4} \right]. \tag{10}$$

These expressions yield the Stokeslet for $t' = \infty$, $r \neq 0$.

The nonslip or perfect-slip condition enters when the constants A and B in Equations (5) and (6) are determined. These constants do not change the characteristics of the dipole and the Stokeslet. We obtain for

Nonslip: $A = -\frac{3}{2}$, $B = \frac{1}{2}$ (Stokes, 1851), (11)

Perfect Slip: $A = -1$, $B = 0$ (Basset, 1888). (12)

The drag for the sphere of unit radius is $6\pi\mu U$ under the nonslip condition, $4\pi\mu U$ under the perfect-slip condition[5].

PROPAGATION OF VORTICITY UNDER PERFECT SLIP

To study the propagation of vorticity by means of diffusion as well as convection under the perfect-slip condition, solutions of the

Navier-Stokes equations are constructed numerically for nonzero Reynolds numbers. The computer program developed to perform the calculations is described in Reference 6. Sufficient notations and remarks are given in the following text such that the reader can understand the results which are presented in Figures 2 through 8.

The computer program is designed to calculate two-dimensional, parallel, unsteady viscous flows of incompressible fluids past elliptic cylinders under various angles of attack. Potential flow is selected as the initial condition, thus simulating the abrupt start of the body. With time either a steady state or a periodic motion develops (for the range of Reynolds numbers under consideration). The infinite flow field is represented by a finite grid system which is based on the elliptic coordinates η and θ defined by

$$x + iy = a \cosh (\eta + i\theta), \; a > 0, \; i^2 = -1. \tag{13}$$

The focal distance is denoted by a, and the body contour is described by $\eta = \eta_1 = 0.1$. Figure 1. The space increments are $\Delta\eta = 0.05$, $\Delta\theta = \pi/30$ or $\pi/40$, and the number of mesh points is $75 \times 60 = 4500$ or $75 \times 80 = 6000$. The Reynolds number is defined by $Re = dU/\nu$, where $d = 2a \cosh \eta_1$. The time t' is made dimensionless by $t' = ta/U$. The computer programs for nonslip and perfect-slip flows differ in the calculation of the surface vorticity, surface velocity, pressure, and the drag, lift, and moment coefficients.

The following cases have been investigated and compared with the corresponding solutions for nonslip flows: (α = angle of attack)

$\alpha = 0^\circ$, Re = 200, symmetric flow, almost steady state, 75 x 60 grid

$\alpha = 90^\circ$, Re = 10, symmetric flow, almost steady state, 75 x 60 grid

$\alpha = 45^\circ$, Re = 200, asymmetric flow, development of vortex street, 75 x 80 grid.

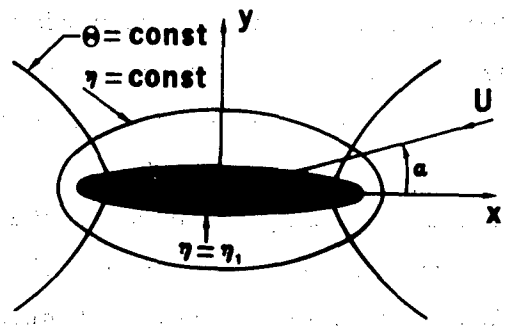

Figure 1 - Elliptic Coordinate System and Definition of Angle of Attack

Surface vorticity and surface pressure along the body contour for symmetric flows are displayed in Figures 2 through 5. Vorticity is more concentrated at the edges for perfect slip than for nonslip. Away from the edges vorticity is almost zero for perfect slip. This reflects the fact that the occurence of vorticity depends on the surface curvature. In the case of the thin elliptic cylinder situated perpendicular to the flow, the surface vorticity changes its sign immediately behind the edges, thus indicating flow separation. The streamline patterns which are presented in Reference 7 verify this and exhibit wakes with twin vortices which are remarkably similar for nonslip and perfect slip. The fact that flow separation occurs for perfect-slip flow is surprising. Obviously, the vanishing of the shear stress at the surface does not prevent flow separation and cannot be used as a criterion for flow separation under the perfect-slip condition. However, the definition for flow separation,

$$\omega_1 = 0, \quad \left(\frac{\partial \omega}{\partial \theta}\right)_1 < 0 \tag{14}$$

based on the vorticity[8] holds for both nonslip and perfect slip.

The peaks in the curves of the surface pressure p_1 at the edges are also more pronounced for perfect slip than for nonslip. Both ω_1 and p_1 are used to compute the coefficients C_D = Drag/ $(\rho/2)U^2d$, C_L = - Lift/$(\rho/2)U^2d$, and C_M = - Torque/$(\rho/2)U^2d^2$. With $C_D = C_{DP} + C_{DF}$,

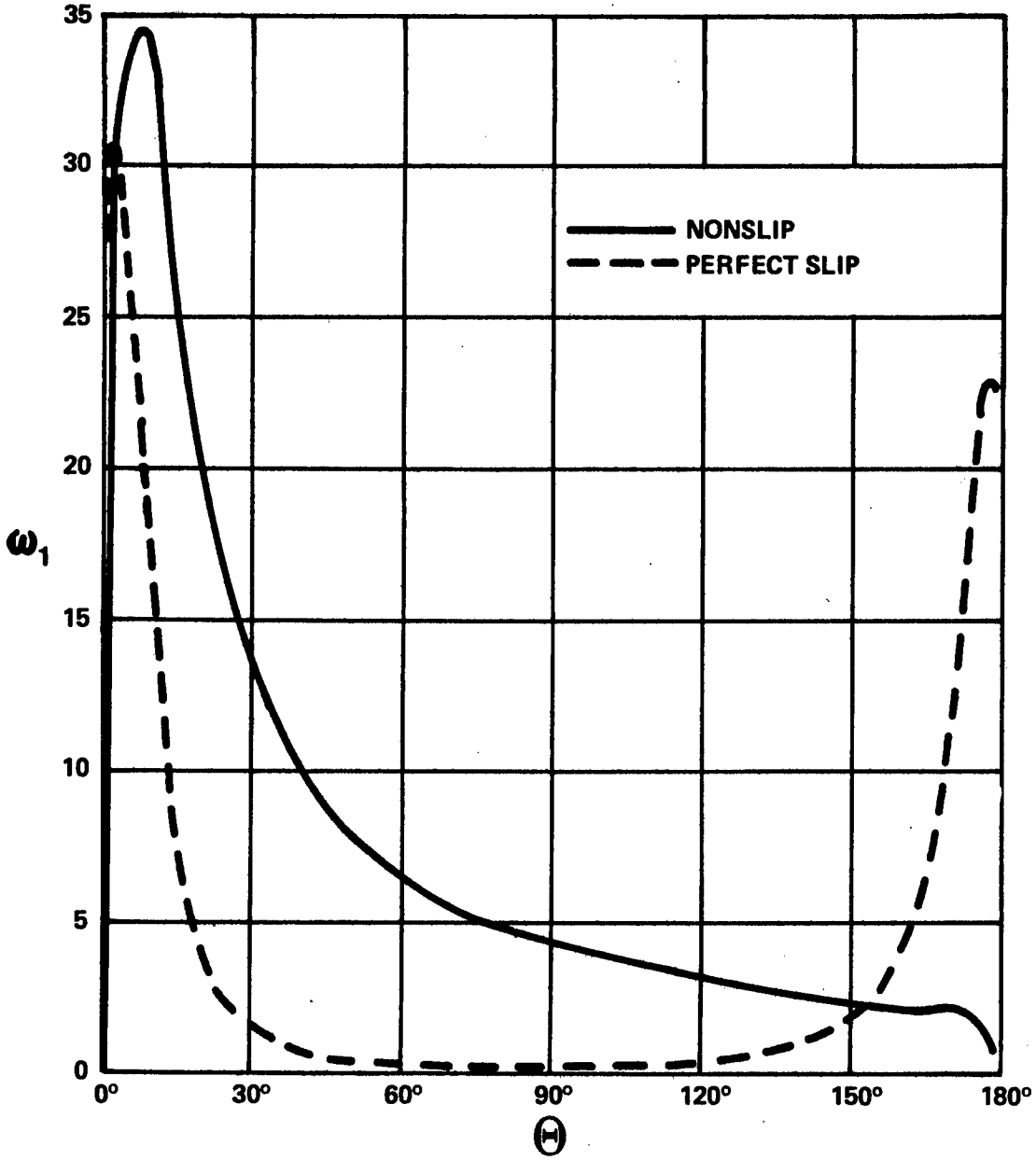

Figure 2 - Surface Vorticity under Nonslip and Perfect Slip for Re = 200, $\alpha = 0^o$, $\eta_1 = 0.1$ at almost Steady State

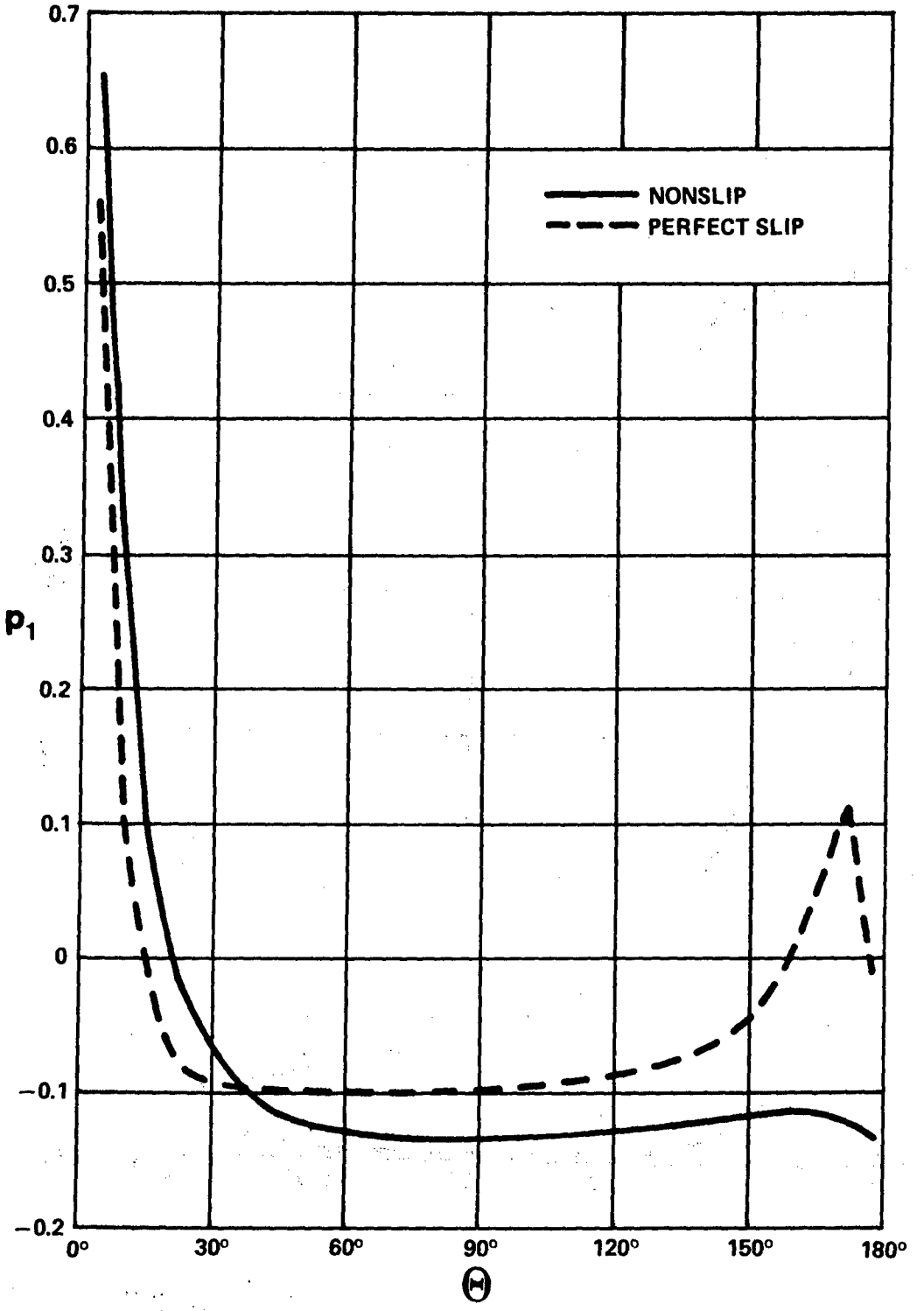

Figure 3 - Surface Pressure under Nonslip and Perfect Slip for Re = 200, $\alpha = 0^o$, $\eta_1 = 0.1$ at almost Steady State

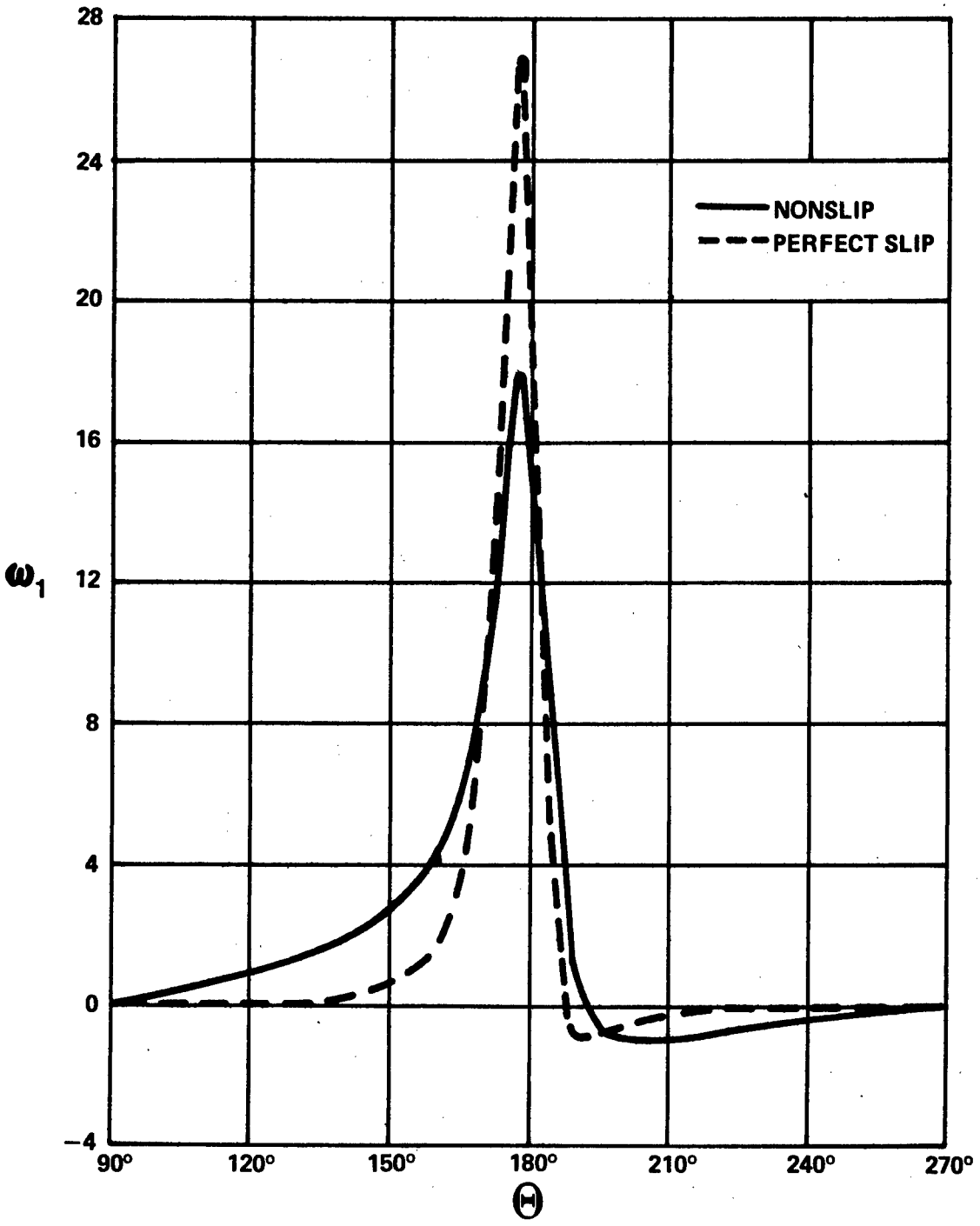

Figure 4 - Surface Vorticity under Nonslip and Perfect Slip for Re = 10, $\alpha = 90^{o}$, $\eta_1 = 0.1$ at almost Steady State

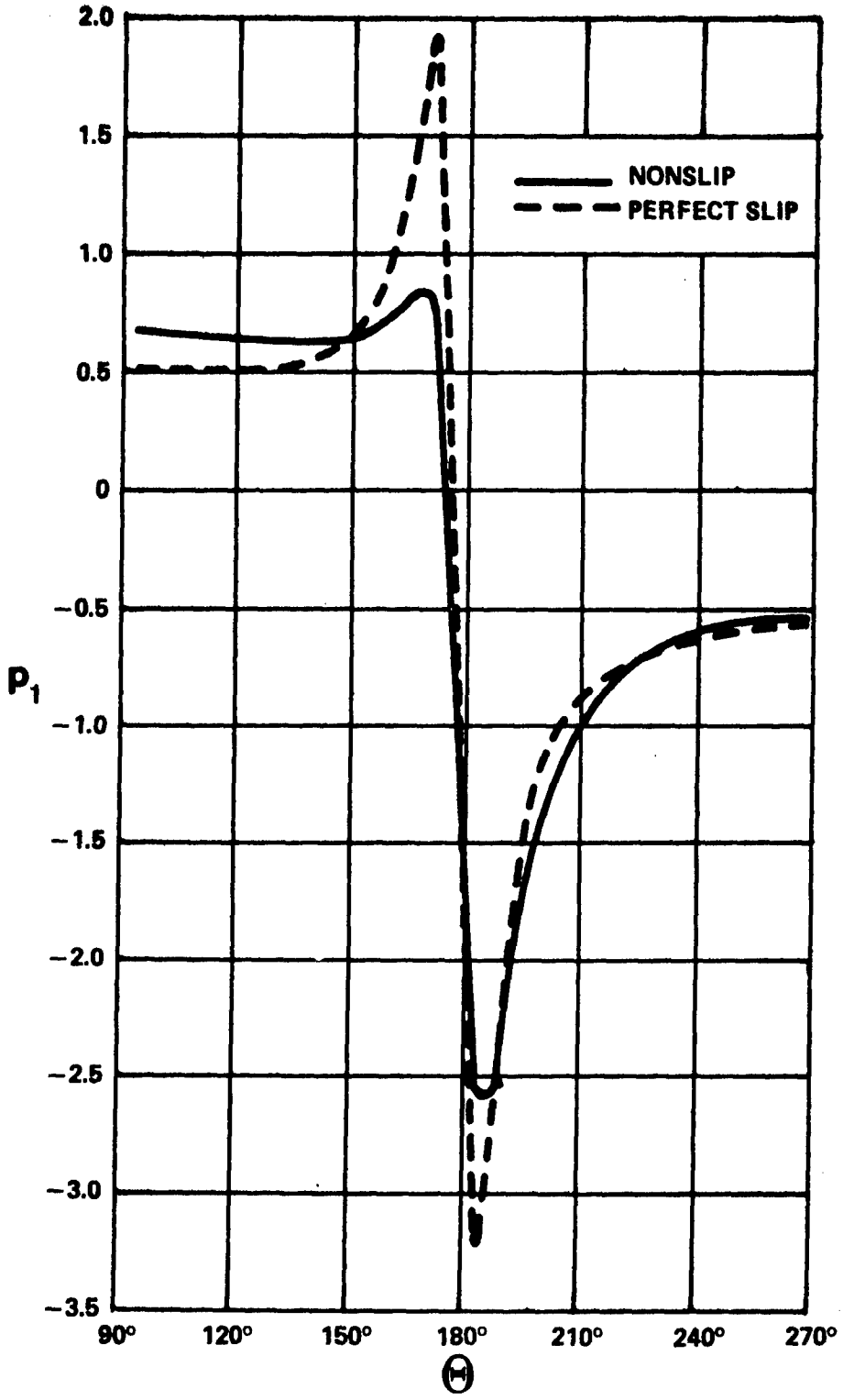

Figure 5 - Surface Pressure under Nonslip and Perfect Slip for Re = 10, $\alpha = 90^{\circ}$, $\eta_1 = 0.1$ at almost Steady State

where C_{DP} and C_{DF} are the drag coefficients due to pressure and friction, respectively, the results are:

$\alpha = 0^{o}$, Re = 200, $\eta_1 = 0.1$: Nonslip $C_D = 0.55$, $C_{DP} = 0.07$

Perfect-Slip: $C_D = C_{DP} = 0.0092$

$\alpha = 90^{o}$, Re = 10 , $\eta_1 = 0.1$, t = 12

Nonslip: $C_D = 6.00$, $C_{DP} = 5.55$

Perfect Slip: $C_D = C_{DP} = 5.73$

Hence, the drag coefficient for the thin elliptic cylinder parallel to the flow decreases 60 times when the nonslip condition is replaced by the perfect-slip condition. However, and this is really surprising, for the elliptic cylinder normal to the flow, the coefficients are almost the same. The reason is that perfect slip reduces drag considerably only for bodies with dominating wall-shear stress. Flow displacement, on the other hand, is scarcely affected by the change in the surface condition.

Once vorticity is produced, it propagates by diffusion and convection, independently of how it is produced. Only in the immediate neighborhood of the surface is propagation directly influenced by the surface condition. Taylor-series expansions around a surface point reveal that only diffusion contributes to the leading terms under the nonslip condition, whereas both diffusion and convection participate when perfect slip is assumed.

The case $\alpha = 45^{o}$, Re = 200 illustrates the behavior of unsteady asymmetric flows under perfect slip. Figures 6 and 7 show patterns of streamlines and lines of constant vorticity for the initial phase of a developing Kármán vortex street. The pictures are remarkably similar for both nonslip and perfect slip except in the central region of the body surface. Under perfect slip an initial vortex is generated as in the nonslip flow giving rise to a flow circulation (in the sense

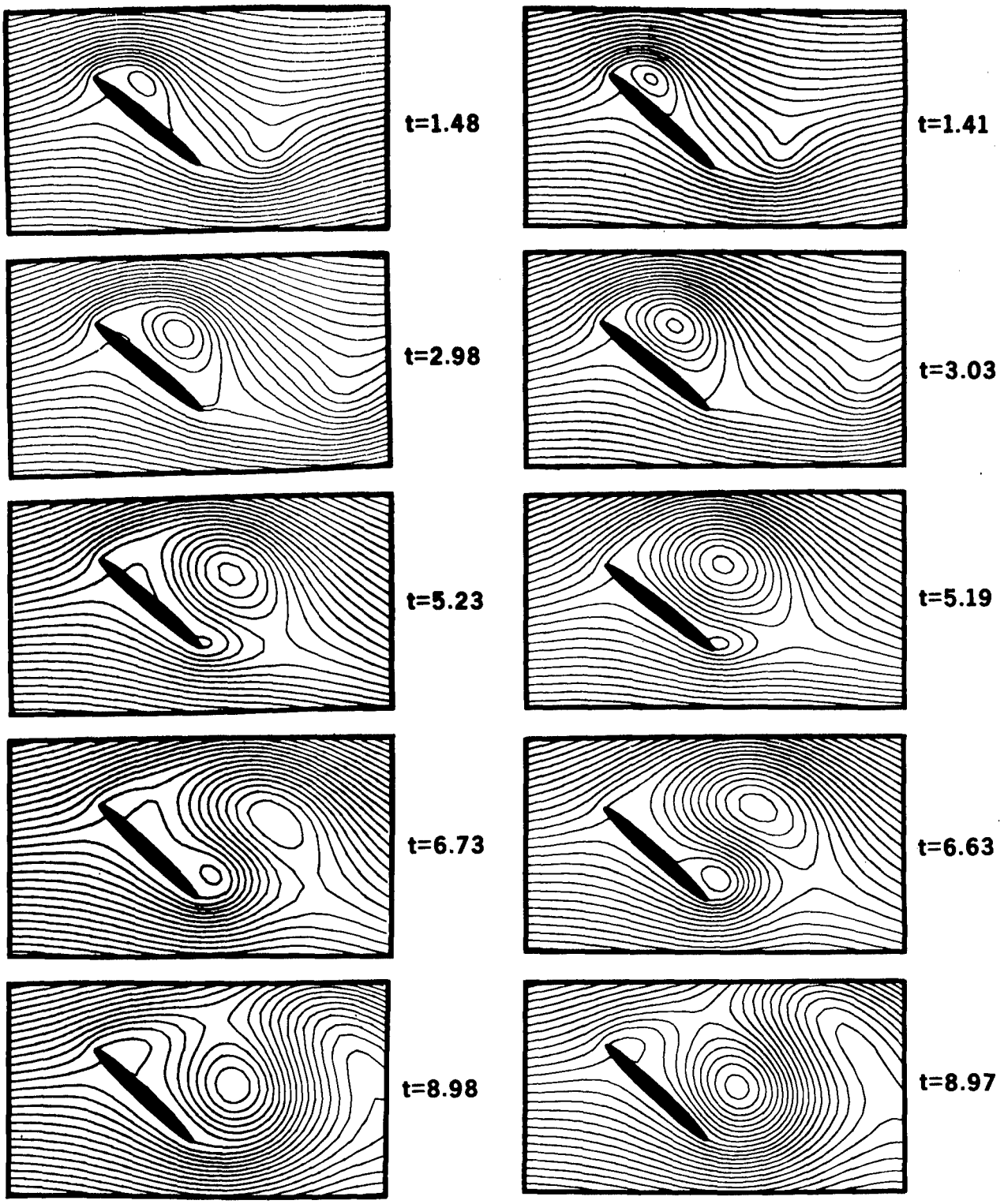

Figure 6 - Sequence of Streamlines for Nonslip and Perfect-Slip Flow after the Abrupt Start of an Elliptic Cylinder with Re = 200, $\alpha = 45^{o}$, $\eta_1 = 0.1$ (Potential Flow at t = 0)

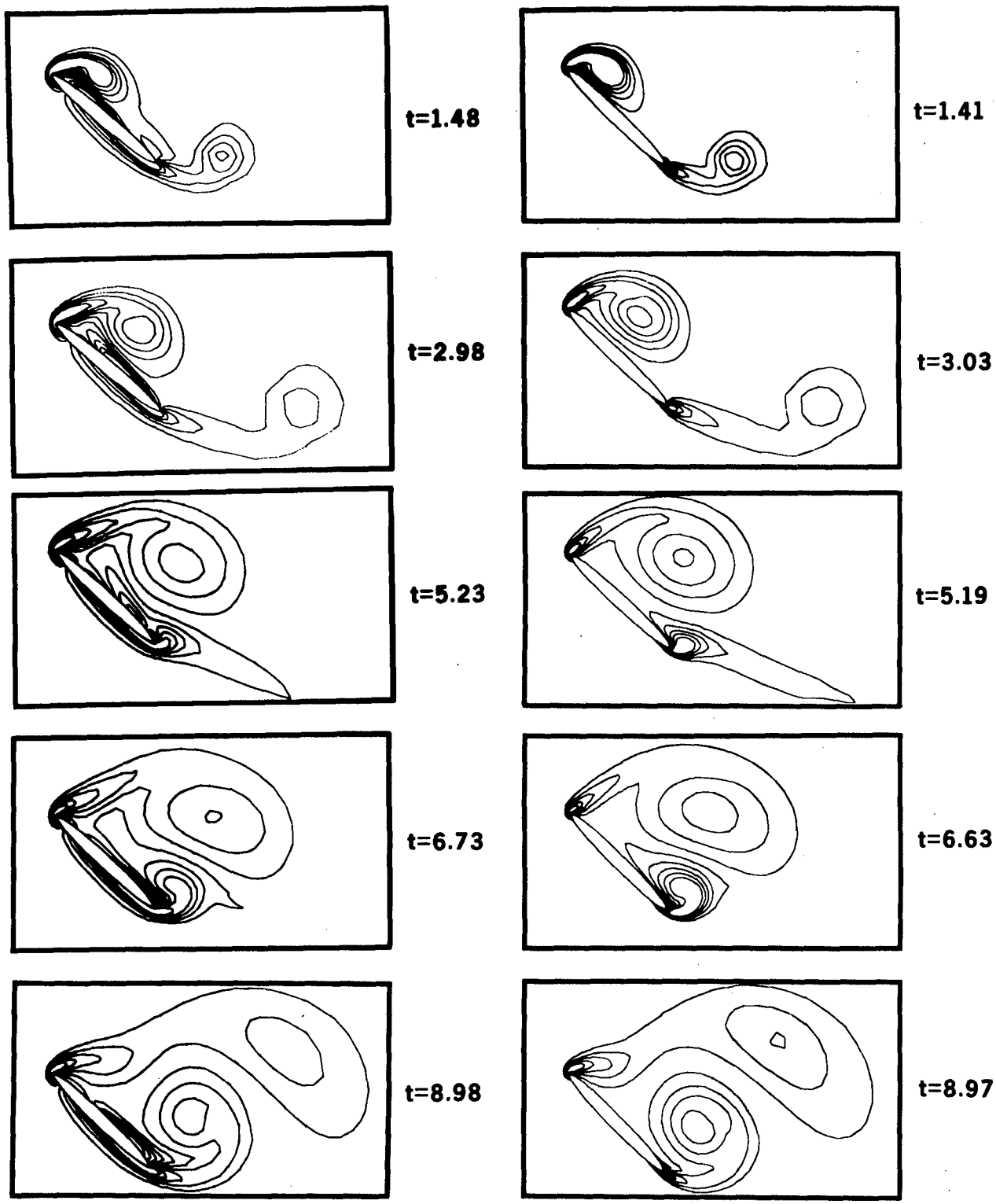

Figure 7 - Sequence of Lines of Constant Vorticity Corresponding to the Streamline Patterns in Figure 6

of the Lanchester-Prandtl hypothesis for potential flow). In Figure 8 C_D, C_L, and C_M are plotted versus t. The orders of magnitude for nonslip and perfect slip are the same. Also the Strouhal numbers[6] agree well. A difference occurs immediately after the start. Whereas for nonslip the sudden start causes infinite values of C_D and C_L and a zero value of C_M, the situation is reversed for perfect slip.

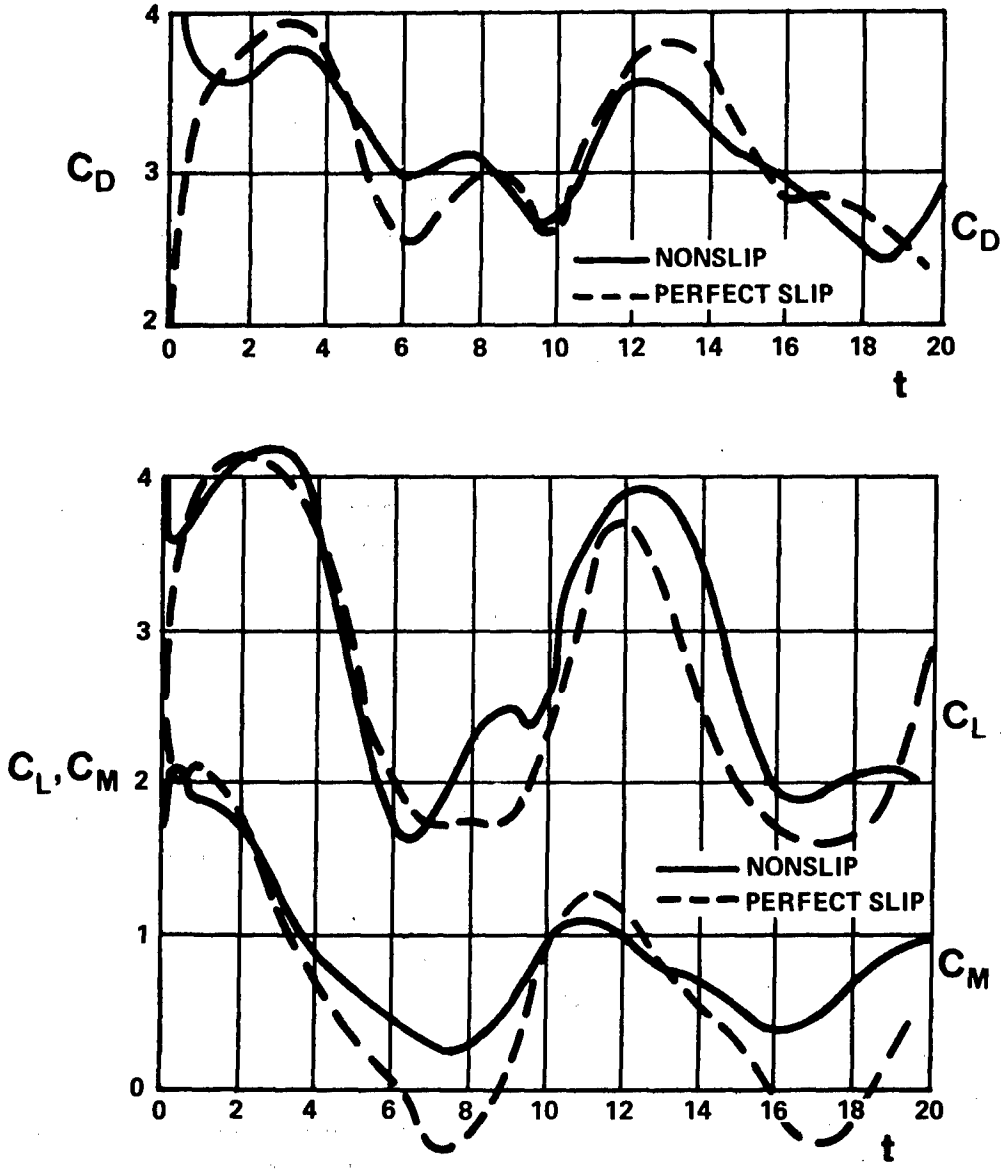

Figure 8 - Drag, Lift, and Moment Coefficients Versus Time for Nonslip and Perfect-Slip Flow with Re = 200, $\alpha = 45^o$, $\eta_1 = 0.1$

ACKNOWLEDGEMENTS

The author would like to thank Professor A. Walz from the Technische Universität Berlin for suggesting the subject and promoting the exchange of information and ideas between the Naval Ship Research and Development Center and Dornier System, Friedrichshafen. The author also wishes to acknowledge the support of Messrs. H. Haussling and S. Ohring in programming the numerical code.

REFERENCES

1. International Symposium on Gas Surface Interactions, to be held at Meersburg, Bodensee, Germany, from May 3-5, 1972, organized by Dornier System, Friedrichshafen.

2. Milne-Thomson, L. M., "Theoretical Hydrodynamics", MacMillan Co., New York, 5th Edition, (1968), p. 648.

3. Phillips, O. M., "The Final Period of Decay of Nonhomogeneous Turbulence". Cambridge Phil. Soc. Proc. 52 (1956), p. 135.

4. Lugt, H. J., "The Spectrum of the Final Decay of Localized Disturbances in a Viscous Fluid". Naval Ship Research and Development Center Rep. 2785 (June 1968).

5. Lamb, H., "Hydrodynamics". Dover publications, New York, 6th Edition (1932), p. 604.

6. Lugt. H. J. and Haussling, H. J., "Laminar Flows Past a Flat Plate at Various Angles of Attack", Proceedings of the Second International Conference on Numerical Methods in Fluid Dynamics. Lecture Notes in Physics 8, p. 78, Springer Verlag. Details are published in Naval Ship Research and Development Center Rep. 3748 (1972).

7. Lugt, H. J., "Vortices and Vorticity Around a Moving Plate", to be published in Scientific American, 1972.

8. Lighthill, M. J., "Laminar Boundary Layers", Editor L. Rosenhead, Oxford University Press 1963, p. 68.

INITIAL DISTRIBUTION

Copies		Copies	
7	CHONR 1 Dr. P. King (102) 1 Mr. M. Cooper (430B) 1 Dr. L. D. Bram (432) 1 Dr. R. D. Ryan (434) 1 Dr. B. J. Macdonald (436) 1 Mr. R. D. Cooper (438)	1	CO, U.S. Naval ROTC & Administrative Unit, MIT
1	DNL	1	Naval War College
1	NRL, Tech Lib	1	NAVSHIPYD BREM
4	NAVSHIPSYSCOM 1 SHIPS 031 1 SHIPS 0311 2 SHIPS 2052	1	NAVSHIPYD BSN
1	NELC, Tech Lib	1	NAVSHIPYD CHASN
1	NURDC, Tech Lib	1	NAVSHIPYD HUNTERS PT
1	NWC, Tech Lib	1	NAVSHIPYD LBEACH
1	NOL, Tech Lib	1	NAVSHIPYD MARE ISLAND
7	NWL 1 Mr. B. Smith (D) 1 Dr. C. J. Cohen (K) 1 Dr. A. V. Hershey (KXH) 1 Dr. E. W. Schwiderski (KXS) 1 Dr. P. Ugincius (KXU) 1 Dr. B. Zondek (KXZ) 1 Tech Lib	1	NAVSHIPYD NORVA
2	SUPT, USNA 1 Dept of Math 1 Tech Lib	1	NAVSHIPYD PEARL
4	SUPT, PGSCHOL, Monterey 1 Lib, Tech Rept Sec 1 Math Dept 1 Dr. T. H. Gawin 1 Prof. T. Sarpkaya	1	NAVSHIPYD PHILA
		1	NAVSHIPYD PTSMH
		12	DDC
		2	U.S. Army Math Res Ctr, Univ of Wisconsin, Madison 1 Dr. D. Greenspan 1 Tech Lib
		1	U.S. Army Res Off, Durham, N.C. 27706 CRD-AA-IPL Box CM
		1	NASA, Wash D. C., Tech Lib
		1	NASA, Marshal Space Flight Ctr Huntsville, Ala 35809, Tech Lib
		1	NASA, Lewis Res Ctr, Cleveland, Ohio 44121

Copies	
3	NASA, Ames Res Ctr, Moffet Field, Calif. 94305 1 Dr. W. J. McCroskey 1 Dr. E. D. Martin 1 Tech Lib
1	NASA, Langley Field, Tech Lib
4	Los Alamos Sci Lab, Los Alamos, New Mexico 87544 1 Dr. F. H. Harlow 1 Dr. C. W. Hirt 1 Dr. B. J. Daly 1 Tech Lib
2	Brookhaven Nat Lab, Upton, Long Island, N.Y. 1 Dr. P. Michael 1 Tech Lib
3	National Bureau of Standards 1 Dr. H. Oser 1 Dr. W. Sadowski 1 Tech Lib
2	Nat Sci Foundation, 1520 H St., N. W., Wash D.C. 20550 1 Engin Sci Div 1 Math Sci Div
4	Princeton Univ 1 Prof. S. I. Cheng 1 Dr. J. Smagorinsky 1 Dr. K. Bryan 1 Aerospace and Mech Eng Lib 1 Prof. M. Kruskal
2	Harvard Univ 1 Prof. G. Birkhoff 1 Prof. F. G. Carrier
4	M.I.T., Cambridge, Mass 1 Prof. J. G. Charney 1 Prof. C. C. Lin 1 Prof. S. A. Orszag 1 Prof. H. P. Greenspan

Copies	
3	University of Md, College Pk, Md. 1 Prof. A. J. Faller 1 Prof. A. Plotkin 1 Prof. D. Sallet
1	USAEC, Tech Lib
1	Oak Ridge Nat Lab., Tech Lib
3	Courant Inst of Math Sci, N. Y. Univ, New York, N. Y. 1 Prof. H. B. Keller 1 Dr. A. J. Chorin 1 Dr. Burstein
2	Stanford Univ 1 Prof. A. Acrivos 1 Prof. M. D. Van Dyke
3	Brown Univ, Prov., R. I. 1 Prof. W. Prager 1 Prof. J. Kestin 1 Prof. M. Sibulkin
2	Poly Inst of Brooklyn 1 Prof. G. Moretti 1 Prof. R. C. Ackerberg
3	Nat'l Cntr for Atmospheric Research, Boulder, Colorado 80301 1. Dr. D. K. Lilly 1 Dr. A. Kasahara 1 Dr. J. W. Deardorff
1	Prof. J. S. Allen, Penn St Univ, Dept of Aerospace Eng, Univ Pk, Pa 16802
1	Dr. J. E. Fromm Dept 977, Bldg 025, Res Div, IBM Corp, Monterey and Cottle Road, San Jose, Calif 95114
1	Dr. C. W. van Atta Univ of Calif, La Jolla, Calif 92037

Copies

1 Dr. E. R. van Driest
North American Rockwell Corp.
350 So. Magnolia Ave, Long
Beach, Calif.90802

1 Prof. W. W. Wilmarth
Univ of Mich, 1077 East Engin
Bldg, Ann Arbor, Mich 48104

1 Univ of Notre Dame
1 Prof. A. A. Szewczyk

2 West Virginia Univ, Morgantown,
West Virginia
1 Prof. J. B. Fanucci
1 Prof. W. Squire

1 Dr. D. Thoman
C23 E. Mishawaha Ave.,
Mishawaha, Indiana

1 Prof. Z. Lavan
Illinois Inst of Tech,
Chicago, Illinois 60616

1 Prof. K. E. Torrance
Cornell Univ, Ithaca, New York

1 Prof. M.Z.v. Krzywoblocki
Mich St Univ., East Lansing,
Mich

1 Dr. W. E. Langlois
IBM Res Lab, San Jose, Calif

1 Prof. J. Happel
Dept Chemical Engin, New York
Univ, New York

1 Hq., American Society of Naval
Engineers, 1012 14th St., N. W.
Washington, D.C. 20005

Copies

1 Dr. M. V. Morkovin
Dept Mechanical & Aerospace
Eng, Ill Institute of Technology
Chicago, Illinois 60616

1 Dr. Vivian O'Brien
The Johns Hopkings Univ
Applied Physics Lab, 8621
Georgia Ave, Silver Spring,
Md., 20910

1 Prof. James C. Wu
School of Aerospace Eng,
Georgia Institute of Tech.,
Atlanta, Georgia 30332

1 Prof. Edmund V. Laitone
Div of Aeronautical Sciences
Univ of California, Berkeley
94720

1 Prof. Raymond E. Goodson
Purdue University, Automatic
Control Center, School of
Mech Eng, Lafayette, Indiana
47907

1 Mr. Stanley K. Jordan
The Analytic Sciences Corp.
6 Jacob Way
Reading, Massachusetts 01867

CENTER DISTRIBUTION

Copies	
1	01
1	15
1	154
1	1541
1	16
1	18
1	1802.2
100	1802.3
1	1805
1	184
5	1843
2	1892

UNCLASSIFIED
Security Classification

DOCUMENT CONTROL DATA - R & D

(Security classification of title, body of abstract and indexing annotation must be entered when the overall report is classified)

1. ORIGINATING ACTIVITY (Corporate author)	2a. REPORT SECURITY CLASSIFICATION
Naval Ship R&D Center Bethesda, Md. 20034	UNCLASSIFIED
	2b. GROUP

3. REPORT TITLE

Generation and Propagation of Vorticity under the Perfect-Slip Condition

4. DESCRIPTIVE NOTES *(Type of report and inclusive dates)*

5. AUTHOR(S) *(First name, middle initial, last name)*

HANS J. LUGT

6. REPORT DATE	7a. TOTAL NO. OF PAGES	7b. NO. OF REFS
February 1972	23	8

8a. CONTRACT OR GRANT NO.	9a. ORIGINATOR'S REPORT NUMBER(S)
b. PROJECT NO.	3794
c.	9b. OTHER REPORT NO(S) *(Any other numbers that may be assigned this report)*
d.	

10. DISTRIBUTION STATEMENT

Approved for Public Release: Distribution Unlimited

11. SUPPLEMENTARY NOTES	12. SPONSORING MILITARY ACTIVITY
	Naval Ship Systems Command

13. ABSTRACT

Renewed interest in slip flow within the realm of continuum physics has resulted in a numerical study on generation and propagation of vorticity in a flow past thin elliptic cylinders under the perfect-slip condition. Computer results show that surface vorticity is more concentrated at the edges for perfect slip than for nonslip, due to the surface curvature. Flow separation, instability, and vortex shedding occur also under the perfect-slip condition. Although drag is drastically reduced for slender body configurations, drag coefficients for a plate normal to the flow are almost the same for nonslip and perfect slip, at least for Reynolds number 10. All computations were carried out for Reynolds numbers below 200.

14. KEY WORDS	LINK A		LINK B		LINK C	
	ROLE	WT	ROLE	WT	ROLE	WT
Perfect Slip Navier-Stokes Equations Vorticity Production						